NASA TECHNICAL MEMORANDUM

NASA TM X-73612

NASA TM X-73612

DESIGN AND PERFORMANCE OF ENERGY EFFICIENT PROPELLERS FOR MACH 0.8 CRUISE

by Daniel C. Mikkelson, Bernard J. Blaha,
Glenn A. Mitchell, and Joseph E. Wikete
Lewis Research Center
Cleveland, Ohio 44135

DESIGN AND PERFORMANCE OF ENERGY EFFICIENT

PROPELLERS FOR MACH 0.8 CRUISE

by Daniel C. Mikkelson, Bernard J. Blaha,
Glenn A. Mitchell, and Joseph E. Wikete

National Aeronautics and Space Administration
Lewis Research Center
Cleveland, Ohio 44135

ABSTRACT

The increased emphasis on fuel conservation in the world has
stimulated a series of studies of both conventional and unconventional
propulsion systems for commercial aircraft. Preliminary results from
these studies indicate that a fuel saving of 14 to 40 percent may be
realized by the use of an advanced high-speed turboprop. This turboprop
must be capable of high efficiency at Mach 0.8 cruise above 9.144 km
(30,000 ft) altitude if it is to compete with turbofan powered commercial
aircraft. Several advanced aerodynamic concepts were investigated in
recent wind tunnel tests under NASA sponsorship on two propeller models.
These concepts included aerodynamically integrated propeller/nacelles,
area-ruling, blade sweep, reduced blade thickness and power (disk)
loadings several times higher than conventional designs. The aerodynamic
design methodology for these models is discussed in this paper. In
addition, some of the preliminary test results are presented which
indicate that propeller net efficiencies near 80 percent were obtained
for high disk loading propellers operating at Mach 0.8.

INTRODUCTION

The increased emphasis on fuel conservation in the world has stim-
ulated a series of studies of both conventional and unconventional pro-
pulsion systems for commercial aircraft (refs. 1 to 13). Preliminary
results from several of these studies, made under NASA sponsorship by
both engine and airframe manufacturers, indicate that the use of an
advanced high speed turboprop propulsion system offers one of the most
promising means of achieving sizable fuel savings and DOC reductions
for future aircraft. A summary of the essential results of these studies
is shown in figure 1 where block fuel consumed and DOC savings are
presented for an advanced Mach 0.8 cruise turboprop compared with both
current and future advanced turbofan powered aircraft. In these studies
a net propeller efficiency of 79.5 percent at Mach 0.8 was assumed along
with an advanced level of technology for the core engine, gearbox, and
propeller structures. As summarized in figure 1, the advanced turboprop

could result in fuel reductions of from 10 to 28 percent for stage length missions from 1296 to 3704 km (700 to 2000 n mi). For a very short mission 185.2 km (100 n mi) a fuel saving of up to 40 percent was projected in reference 7. In addition, an advanced turboprop could result in DOC saving of from 3 to 5.3 percent assuming 8¢/liter (30¢/gal) fuel or from 4.5 to 8.2 percent for 16¢/liter (60¢/gal) fuel.

This advanced turboprop must be capable of high efficiency at Mach 0.8 cruise above 9.144 km (30,000 ft) altitude if it is to compete with turbofan aircraft. In the past it was known that propellers were highly efficient at cruise speeds up to approximately Mach 0.65. However, above this speed large compressibility losses on the propeller blading caused the efficiency to fall rapidly. This lower efficiency at higher speeds combined with a high maintenance burden for the early turboprops contributed to the rise of the turbojet and turbofan propulsion concepts for the higher speed commercial aircraft. Because of the success of the turbojet and turbofan, little was done to improve propeller performance for higher cruise speeds. However, with the oil shortage of late 1973 NASA Lewis Research Center along with Hamilton Standard conducted several studies to explore the energy saving potential of applying advanced aerodynamic and structural technology to the high speed propeller. Some of the aerodynamic concepts that were evaluated are discussed in references 14 and 15 and include: highly integrated propeller/nacelles, blade tip sweep, area-ruling, reduced blade thickness, and advanced airfoils. In addition, to hold propeller diameters to a reasonable value for Mach 0.8 cruise above 9.144 km (30,000 ft) altitude power (disk) loadings several times higher than conventional designs are required. These high loadings then would require increasing the number of propeller blades. From the initial results of these studies (ref. 15) it was estimated that an advanced turboprop can be designed with installed propulsive efficiencies at Mach 0.8 cruise that would be about 15 percent higher than the best advanced turbofan (fig. 2). An artist sketch of a typical advanced Low Energy Turboprop Transport is shown in figure 3.

In support of these early studies of high speed propellers two advanced propeller models were designed and wind tunnel tested to evaluate their performance. Several of the advanced aerodynamic concepts were incorporated in the design of these models. This work was done by Hamilton Standard under contract to NASA Lewis Research Center. Initial results from these tests are presented in reference 15. It is the purpose of this paper, therefore, to discuss the aerodynamic design methodology for these models and present some of the more interesting test results. This work discussed above has been directed toward energy conservation for advanced commercial aircraft, however, the results that will be covered in this paper should also be applicable to the higher performance business aircraft.

THEORETICAL ADVANTAGES OF TURBOPROPS

The inherent theoretical advantages of a turboprop propulsor can be demonstrated from simple momentum theory. Ideal propulsive efficiency is shown in figure 4 as a function of fan pressure ratio which is analogous to power loading These curves were derived for flight Mach numbers from 0.1 to 0.8 using simple momentum theory and represent only the induced axial loss The calculations assumed an adiabatic fan efficiency of 1.0 and included no viscous losses. The ranges in fan pressure ratio typical for each type of propulsor are indicated. Conventional propellers generally were lightly loaded with fan pressure ratios up to about 1.03. Advanced propellers require more power to fly at higher speeds. Also, because of the low air density at the higher cruise altitudes, a higher power loading is required to keep the propeller diameter to a reasonable size. Fan pressure ratios for the higher-loaded advanced propellers will range from about 1.03 to 1.07. High bypass ratio turbofans are more highly loaded with fan pressure ratios generally greater than 1.3.

The design point established for the initial advanced turboprop engines included a power loading of 301 kW/m^2 (37.5 SHP/D^2) at 243.8 m/sec (800 ft/sec) tip speed and 10.668 km (35,000 ft) altitude. These conditions resulted in a design integrated fan pressure ratio of 1.047. In terms of power loading 301 kW/m^2 (37.5 SHP/D^2) is about three times the loading used on previous conventional propeller aircraft such as the Lockheed Electra/P-3. A typical advanced turbofan of comparable technology is projected to have a fan pressure ratio of about 1.6. Therefore, from figure 4, the ideal efficiency for the advanced turboprop at Mach 0.8 cruise would be 97 percent, while that for the comparable turbofan would be 80 percent. The turboprop exhibits therefore an inherent 17 percent benefit. As seen in figure 4 this ideal advantage would be larger at lower flight speeds.

The simple momentum theory however does not account for the residual swirl loss in the propeller wake. This swirl is a loss that is unique to a propeller since it is not recovered by stators as it would be in a fan engine. Therefore, the ideal propeller efficiency shown in figure 4 has to be corrected for this loss. The swirl loss is shown in figure 5 by comparing the basic axial momentum loss with the total induced loss for a configuration with an infinite number of blades. This loss is shown in figure 5 in terms of ideal propeller efficiency as a function of power loading. At the power loading selected for the propeller design (which will be discussed later) the swirl represents about 7 percent performance penalty. However, it should be possible to eliminate a large part of this penalty if counter rotation propellers are considered. This more mechanically complex approach is being considered as an alternate propulsion concept for the advanced turboprop, however, it will not be covered in this paper.

A further correction also has to be made for propellers which is associated with tip losses for a finite number of blades. Figure 5 shows that tip losses increase dramatically as the number of blades is reduced. At the higher power loadings the tip losses with two or four blades are excessive. With an eight blade propeller the tip losses are tolerable. For any number of blades, propeller efficiency increases as power loading is decreased. But such an increase in aerodynamic efficiency would require larger propeller diameters and thereby in-crease blade and gearbox weight. These considerations resulted in an eight blade propeller with a power loading of 301 kW/m² (37.5 HP/ft²) for an initial design. The tip loss for this design is nearly 5 percent and the total loss (swirl and tip) above the axial momentum loss is about 12 percent. However even with these two additional penalties, it is evident from figures 4 and 5 that the highly loaded turboprop at Mach 0.8 still shows a significantly higher ideal efficiency than the high fan pressure ratio turbofan (85 percent vs 80 percent). This advantage for the turboprop would be considerably larger if the turbofan performance was adjusted for fan losses due to fan adiabatic efficiency, inlet recovery, nozzle efficiency, and cowl drag.

DESIGN OF ADVANCED PROPELLERS

Several advanced aerodynamic concepts need to be considered if a propeller is to achieve a high level of efficiency for cruise at Mach 0.8 above 9.144 km (30,000 ft). A summary of some of the more important aerodynamic concepts is shown in figure 6. These concepts include: the use of reduced blade thickness and sweep to minimize compressibility losses; tailored nacelle blockage and spinner area-ruling to reduce the flow velocity through the blading to minimize choking and particularly compressi-bility losses in the blade roots; and lastly, the use of advanced airfoil technology. When studied individually all of these concepts theoretically indicate some benefit, however very few have been adequately investigated. To realize the performance benefits required, several or all of the above concepts may have to be employed successfully. A further discussion of each of these concepts will be made in the following paragraphs.

The advantage of reduced blade thickness on reducing compressibility losses is explained using figures 7 and 8. Figure 7 shows three blade thickness distributions that were wind tunnel tested back in the mid 1950's using lightly loaded two-bladed propeller models. For reference the blade with the intermediate thickness (t_2) was close to the thickness distribution of the Lockheed Electra/P-3 propeller. The blade with the lowest value of thickness distribution (t_1) had a thickness of 2 percent at the tip. Full scale construction of a thin blade such as t_1 was not possible in the 1950's. At that time fabrication was limited to all metal blades. However, with advanced fabrication technology using the composite spar/shell concept thin blade construction (i.e. t_1) should be possible in the future. Figure 8 shows the maximum efficiency observed for each of the three blade thickness distributions as a function of Mach number. The maximum efficiency for each was fairly high at Mach

numbers below 0.7 However at higher speeds the efficiency dropped
rapidly except for the thinnest propeller (t_1) which had a peak efficiency
of 82 percent at Mach 0.8. These results are a consequence of the fact
that the drag rise Mach number is higher for thinner airfoil sections.
However, it should be noted that propellers are not generally run at
their maximum efficiency condition since, as will be seen later in the
data, the power absorbed is too low from a propeller weight standpoint.
The trends demonstrated with these data are significant however since they
show the definite advantage of thinner blades at the higher cruise speeds.

Blade rotary tip speed is selected based on a compromise between
aerodynamics and acoustics. At cruise conditions high tip speeds result
in lower induced losses, however, if tip relative Mach numbers significantly
exceed Mach 1 blade drag losses increase and high noise may result.
At takeoff, a subsonic tip speed is required to keep airport community
noise low. Based on these considerations a tip speed of 243.8 m/sec
(800 ft/sec), for takeoff and cruise, was selected for the initial advanced
turboprop design. This tip speed results in a relative tip Mach number
of 1.14 at Mach 0.8 cruise.

The concept of blade sweep in a propeller design relies on the
simple cosine rule which reduces the effective Mach number at a blade
section as a function of the sweep angle. Increased cruise performance
may be possible with sweep because the blade leading edge can be kept
subsonic and thereby reduce shock strength and lower compressibility
drag. Since the noise of high tip speed propellers is influenced by
blade shock strength, sweep might also reduce cruise noise. The use
of advanced supercritical blade sections in a high tip speed propeller
design would also require sweep to keep the rather blunt blade sections
at a subsonic speed where they could produce superior lift-to-drag ratios.

The technique of designing sweep into a propeller blade can be shown
using figure 9. This figure shows relative Mach number across the span
of the propeller blade from hub-to-tip for a 243.8 m/sec (800 ft/sec) tip
speed at Mach 0.8. Curve A shows relative Mach number without sweep
(i.e. a straight blade) and should be compared to curve B which shows the
drag-divergent Mach number for each radial location. Curve B is for
NACA 16 series blade sections with a thickness distribution similar to t_1
of figure 7. This comparison shows that essentially all of the blade
sections are into drag rise. In addition, the tip relative Mach number
is up to 1.14. Curve C shows the effective Mach numbers for a propeller
blade with about 30° of sweep. Outboard of the 0.6 radius station the
blades are swept just enough to keep the Mach number below drag rise
Inboard of this station some suppression of the local flow field would be
needed to keep the blade sections below drag rise. Nacelle blockage and
spinner area-ruling, therefore, are concepts that can be applied to this
region of a high speed propeller. Proper contouring of the spinner and
nacelle can signficantly reduce the axial Mach number in the hub region
of the propeller as shown in figures 10 and 11. Figure 10 shows the local
surface Mach number and figure 11 the Mach number near the propeller

leading edge calculated using the potential flow method of reference 17 for a nacelle diameter equal to 35 percent of the propeller diameter. Local surface Mach numbers approaching 0.6 were calculated for a free-stream Mach number of 0.8. A transonic flow program (ref. 18) and a compressor program (ref. 19) have also been used to analyze this region of the propeller. The nacelle geometry of figure 10 does result in some local supercritical flow near the maximum nacelle diameter. In order to keep nacelle drag low the peak local Mach number should be kept below approximately Mach 1.3 based on experience with turbofan nacelle cowlings (ref. 20). The effect of this flow field suppression on blade relative Mach numbers is shown by curve D of figure 9. An eight-blade propeller would have gap to chord ratios less than one in the hub region and therefore would be subject to cascade effects. Also, with this close blade spacing and very thick blade sections in this region local flow choking could be a serious problem. However, by carefully area ruling the spinner in the blade root region this potential problem should be minimized.

The basic design procedure for an advanced high speed propeller with a high power loading has become a rather complex blend of conventional propeller design techniques, modified to incorporate some of the advanced aerodynamic concepts discussed earlier in combination with compressor design procedures. A block diagram or flow chart illustrating the current design procedure is shown in figure 12. This procedure begins with a preliminary analysis where the propeller diameter, number of blades, RPM, and power are selected. Blade thickness distribution is generally chosen, as mentioned earlier, as the minimum allowable by stress limitations, aeroelastic considerations, and the fabrication state-of-the-art. The initial blade planform (chord distribution or activity factor) is selected based on experience and a preliminary performance analysis of the design condition. With the selection of the initial propeller geometry and design operating conditions; along with a blade leading edge velocity gradient (from the spinner/nacelle calculations); the propeller is analyzed using a conventional strip integration program. This program is based on the work of Goldstein (ref. 21) and has been modified to accept velocity gradient inputs. Some of the other details of this program and its limitations will be discussed later. With this program the designer attempts to optimize induced efficiency and profile efficiency. The induced efficiency is optimized by using the optimum (Goldstein) blade loading distribution at the design point. With this loading, the designer attempts to minimize blade profile drag losses by iterating between angle of attack and camber. As mentioned earlier the blades are very thick and close together in the hub region, therefore cascade effects are important and choking could be a potential problem. The flow in this region is analyzed and cascade airfoils are selected using compressor programs similar to those of references 22 and 23. The propeller design must now be checked at takeoff and climb conditions. Because good low speed performance requires high camber, the low camber blades designed for high speed cruise generally need to be modified to a slightly higher camber. The inclusion of both the

hub design and takeoff constraints requires additional iterations of the Goldstein strip analysis program to insure that the final design has the highest cruise performance with adequate takeoff performance Future propeller design and analysis programs, hopefully, will analyze the total propeller/nacelle flow field with a fully integrated capability.

Since the Goldstein strip integration program is the basic tool that is used in this design procedure, it is worth examining how the early work of Goldstein has been extended and also discuss some of the program limitations. As was mentioned earlier, this program has been modified to accept local Mach number distributions associated with nacelle and spinner flow field suppression. This is done by calculating the induced velocity at each strip separately assuming uniform flow to the propeller at the local strip Mach number. The current program uses compressible airfoil data for the high speed design case. Also, the analysis has been modified to incorporate a cascade correction in which the zero lift angle and the lift curve slope of the airfoil data is modified depending on the local gap-to-chord ratio. Another correction accounts for three-dimensional "tip relief" (of compressibility losses) that depends on local tip aspect ratio This correction is based on the data of reference 24. The blade sweep routine in the program applies simple cosine rule treatment to the airfoil data and local velocity field.

There are some areas where the Goldstein analysis does not correctly represent the true flow field. This analysis uses a straight lifting line normal to the axis of rotation. When it is applied to a swept blade the induced flow velocity and resulting blade loading distribution are not correctly represented. This limitation can result in the prediction of too high a loading in the outboard region of a swept blade. In addition, propellers with tips at supersonic speeds will produce reduced induced flow near the tip region due to the zone of influence which is limited by the acoustic velocity (ref. 25). This results in the Goldstein program predicting too low a loading in this region. In contrast to this effect, reference 26 predicts that wing tips in supersonic flow will lose lift. This reduction in loading may cancel out some of the difference associated with the underprediction of the tip loading due to the induced flow reduction. Of these three effects only the reduced induced flow effect (associated with supersonic tip speeds) was incorporated into the initial two high speed propeller designs by use of the Biot-Savart equations (pps. 67-69 of ref. 25). Since some of the effects discussed above result in mutually cancelling trends the inclusion of a single effect may not be the best design approach.

In the design of the two initial advanced turboprop configurations, Hamilton Standard used the above design procedure, including the Biot-Savart equations in an attempt to further optimize the Goldstein blade loading. The first, designated SR-1, utilized a blade with about 30 degrees of sweep at the tip; and the second, designated SR-2, was for a straight blade. The characteristics of the swept blade, SR-1, are shown in

figures 13(a) and 13(b), and those of the straight blade, SR-2, are
shown in figure 13(c). The thickness and chord distributions of both
blades were identical. The blades differed somewhat in camber and
twist distributions due to differences in sweep and spinner geometry.
SR-1 had a conical spinner and SR-2 had an area ruled spinner. Both
used NACA 16-series airfoil sections in the outboard regions. The SR-1
utilized NACA 65-series blades in the hub region whereas the SR-2
utilized a modified 65-series having a circular arc mean camber line.
In general, except for sweep, SR-1 and SR-2 were similar. The
resulting design characteristics for both were identical as shown below:

   0.8 Cruise Mach Number
   10.668 km (35,000 ft) Cruise Altitude
   8 Blades
   203 Activity Factor Per Blade
   301 kW/m^2 (37.5 HP/ft^2) Power Loading
   243.8 m/sec (800 ft/sec) Tip Speed
   0.08 Integrated Design Lift Coefficient

Because a variation of the Goldstein program was not used in the design
procedure the swept blade loading shown in figure 14 is not the classical
Goldstein loading; but it is similar to it. The straight blade con-
figuration also had a similar loading distribution. Because of the
straight tips the calculated compressibility losses were higher for this
blade and the calculated design net efficiency was only 77 percent in
contrast to 79.5 percent for the swept blade.

WIND TUNNEL MODELS AND TESTS

The design procedures discussed above were used by Hamilton Standard
to generate two initial advanced turboprop configurations. The first
utilized a swept blade approach and the second a straight. Under contract
to Lewis, Hamilton Standard then fabricated these two into 62.23 cm (24.5 in.)
diameter scale wind tunnel models. The two models are shown in figure 15
installed on a 373 kW (500 HP) propeller test rig (PTR) in the United
Technology Research Center (UTRC) Large Subsonic Wind Tunnel. The PTR
is powered by two electric drive motors and included a force balance
for measuring propeller thrust and a torque meter for shaft power. The
models were composed of the blades, spinner, and a simulated axisymmetric
nacelle. The swept configuration is shown in figure 15(a) and the straight
blade configuration in figure 15(b). As can be seen in figure 15 the swept
blade configuration had an approximate conic spinner with blade root
platforms and the straight blade configuration had an area-ruled spinner
without platforms. Root platforms were used with the conic spinner to
facilitate a wider range in blade angle (β 3/4) capability. With the
platforms blade angle could therefore be varied from reverse thrust
through feather (-8° to $\sim$ 90°+) without contacting the spinner. The conic
spinner/nacelle combination was designed initially, as discussed in the
previous section, to suppress the local flow field near the blade leading

edge. The area-ruled spinner concept was thought of later and therefore was used only on the second model. Both propellers used the same nacelle geometry which had a ratio of maximum diameter to propeller diameter of 0.35.

A comparison of the two blade configurations is shown in figure 16 and the detailed aerodynamic and geometric design characteristics for each blade were shown previously in figure 13. By comparing the details in figures 13(a) and (c), and the photograph (fig. 16) it is evident that the two configurations were essentially the same except the SR-1 included 30° of aerodynamic sweep at the tip.

The wind tunnel tests were conducted at zero model incidence to the flow over a range in Mach number from 0.15 to 0.85. Blade angle, (β 3/4), which is defined at the radius ratio station, (r/R), of 0.75, was varied at each Mach number.

TEST RESULTS

Wind Tunnel test results are presented in figures 17 through 21. In figures 17 and 18 data are presented from the swept blade configuration (SR-1) and in figures 19 and 20 from the straight blade configuration (SR-2). A summary of the more pertinent cruise results is presented in figure 21.

In figure 17 net efficiency (η_{net}) and power coefficient (Cp) are presented for the swept blade model (SR-1) at the design cruise Mach number ($M_0 = 0.8$) and low speed ($M_0 = 0.2$). Data are presented for a range of blade angle (β 3/4) at each Mach number. The analytical predicted performance point for each speed is also shown as a solid symbol. As mentioned previously the analytical design point for the swept blade would yield an efficiency of 79.5 percent at an advance ratio ($J = 3.06$) and power coefficient of (Cp = 1.7) As mentioned previously this design point does not exist at the advance ratio (J) where the maximum efficiency would be expected. As seen in the data at the maximum efficiency the power absorbed is low. The predicted blade angle was 56°, but as seen in figure 17(a), an experimental value 5 higher (61°) was required to achieve the design power. Similar results were observed at low speed, however the blade angle difference was only 3° A crossplot of the performance data is presented in figure 18 as a function of power loading (SHP/D^2). In figure 18(a) the cruise net efficiencies of figure 17(a) are presented for a 243.84 m/sec (800 ft/sec) tip speed (at Mach 0.8). At the design power loading the experimental efficiency was 77 percent compared to the calculated value at this condition of 79.5 percent When the gaps between the blades and spinner platforms (fig. 15) were faired over and sealed the experimental performance increased to about 78.2 percent, but was still below the predicted value Experimental values of net efficiency did exceed 80 percent with the swept blades at lower power loadings. However, shifting the design point to

lower power loadings may not be desirable since this would result in larger propeller diameters and in higher propulsion system weights.

The low speed results shown in figure 18(b) were converted into a thrust to power ratio which is more appropriate for analyzing takeoff performance. This has been done since the efficiencies at these speeds are very low (< 50 percent) and the significance of advance ratio is lost at the low forward speeds. These results are again shown as a function of power loading for sea level operation. At low speed the data are in contrast with the cruise results. At the design power loading the experimental thrust exceeded the analytical prediction value by about 10 percent. This result was also indicated in figure 17(b) where the experimental efficiencies exceeded the analytical prediction.

In summary the results observed with the swept blade configuration indicate that at cruise and takeoff fairly high performance can be obtained but the analytical predictions do not agree well with experiment. These differences observed between the analytical and experimental results will be discussed further when the results of the two blade configurations are compared and summarized.

Performance data for the straight blade propeller (SR-2) are presented in figure 19 for Mach 0.8 cruise (fig. 19(a)) and Mach 0.2 (fig. 19(b)). The design points for each condition are also shown as solid symbols. At Mach 0.8 cruise an efficiency of 77 percent at a blade angle (β 3/4) of 56.8° was predicted. At low speed the design blade angle was 35.5°. An experimental blade angle of about 58° was required to obtain the cruise power and about 38.5° to achieve the low speed condition. The 1.2° difference seen at cruise is much closer to the predicted angle than was the SR-1 configuration and is within the capability of the current design procedures. Figure 19 also shows that the efficiencies measured with the straight blade at M_0 = 0.8 cruise were higher than predicted and in general exceeded 80 percent.

As with the swept SR-1 model the performance data are shown cross-plotted in figure 20 as a function of power loadings. At Mach 0.8 cruise, data for several tip speeds are shown. At the design power loading of 301 kW/m² (37.5 SHP/ft²) and tip speed 243.8 m/sec (800 ft/sec) the experimental efficiency was 78.8 percent in contrast to the calculated value of 77 percent. This somewhat high experimental efficiency is not completely understood at this time. Because of the straight blades and high tip Mach number of 1.14 this configuration was predicted to have more compressibility loss than the swept blade configuration. However, one contributing factor may have been the influence of the area-ruled spinner on this configuration.

Because of the relatively high experimental performance of the straight-blade propeller, its operation at off-design conditions was investigated and shown in figure 20(a) at other tip speeds. An efficiency of 80.2 percent was obtained at the design power loading with a tip speed

of 259 m/sec (850 ft/sec). The data also show that greater increases in efficiency may be obtained for lower tip speeds. The low speed results (fig. 20(b)) again indicate that the experimental performance with the straight blade slightly exceeded prediction.

A summary of the cruise performance at 0.8 Mach number is shown in figure 21 for both the swept (SR-1) and straight-blade (SR-2) configuration. Comparisons are made between the experimental results of the two configurations and also the analytical predictions. For the straight-blade configuration the experimental results show that the design performance was exceeded and the blade calculated design angle was obtained within the design procedure capabilities. The results were just the opposite with the swept blade. The experimental efficiency fell below prediction and the blade set angle was off by 5°. During the tests with the swept blades flow visualization and wake survey data were obtained. These data also indicate that the swept blades were not performing as designed. The wake survey measurements indicated that the loading at the design blade angle was considerably less than originally predicted This was especially true in the tip region. To compensate it was necessary to increase the blade angle by 5° to achieve the desired power loading. This resulted in an overloading of the blades in the inboard regions. The flow-visualization data also indicated a possible flow separation at the trailing edge in the mid-span regions of the blades. It appears at this time that the problems associated with the swept blade lie with the inability to properly account for the effects of tip sweep and not with the concept of sweep. As discussed in the section on Advanced Propeller Design the techniques used are not complete and are not unified into an integrated design procedure.

The comparisons shown in figure 21 for the off-design condition with the straight blade (SR-2) indicate however that the high propeller efficiencies required to obtain the block fuel and DOC savings projected in the mission analysis studies of references 1 to 13 should be obtainable. In addition, a further analysis of the test data along with an examination of all propeller loss mechanisms, indicates that it may be possible to obtain propeller efficiencies that approach 82 percent at the same design condition. This level of performance would result in even larger fuel savings and DOC advantages.

POTENTIAL PERFORMANCE IMPROVEMENT AREAS

The very encouraging results of the two initial tests have stimulated further studies. From these tests and studies it has become apparent that there are several areas where potential performance improvements may be obtainable. A list of these areas is shown in figure 22. Foremost among these items is the need for an updated, comprehensive design analysis Current analyses methods have become inadequate especially when the aerodynamics become complicated as with the transonic flow over the swept-blade. An updated analysis would more accurately predict the blade

geometry to give an optimum loading.

Included in the list of items that were utilized with the initial configurations are revised twist, cleaner blade root fairing and sealing, improved sweep, advanced (supercritical) blade section technology, improved spinner/nacelle tailoring and area-ruling, and improved thickness distributions. Some of these items were incorporated to some degree. in the first two designs and are the primary reason for the high performance that was observed. However more work can be done on each of these to arrive at an optimum configuration. Other items that were not utilized on these two initial designs include increased blade numbers, lower design power loadings, and the use of counter rotation.

The last item mentioned in figure 22 is probably the most difficult to employ but shows promise of having the largest potential performance benefit. Figure 5 showed that there was a 7 percent swirl loss with the current single rotation propeller designs. With the use of counter-rotation recovery of at least half (or more) of this loss may be possible.

FUTURE TESTS

To further explore some of the potential performance gains listed on figure 22, NASA Lewis Research Center is planning to investigate several advanced single and counter-rotation propeller models. This work is planned to be done in support of the NASA Advanced Turboprop Program (FY 1978 new program). The single rotation models will be tested on the NASA Lewis Research Center 745.7 kW (1000 HP) Propeller Test Rig shown in figure 23. This rig incorporates a small 6-inch diameter air turbine and a rotating balance (located directly behind the test propeller) to measure thrust and torque.

CONCLUDING REMARKS

For the advanced turboprop to be competitive with proposed advanced turbofan engines it must demonstrate high propulsive efficiency at Mach 0.8 cruise above 9.144 km (30,000 ft) altitude. This goal will require the incorporation of several advanced aerodynamic concepts. A propeller for this advanced turboprop needs to be designed integrally with the local nacelle flow field and take advantage of all the aerodynamic suppression possible to overcome the inherent compressibility losses at these high cruise speeds. The two initial models were designed to employ several of these aerodynamic suppression concepts. Results from these first two configurations were very encouraging and demonstrated the potential for meeting, and possibly exceeding, the performance goal of 80 percent efficiency at Mach 0.8 cruise. Results from the swept blade (SR-1) indicate that more effort is required to properly incorporate sweep so that the estimated aerodynamic performance gains may be realized. Similarly, work is planned to evaluate the potential benefits of counter-rotation, which may exceed the maximum performance expected from single

rotation. In addition, any future commercial turboprop aircraft must have a cabin environment equivalent in ride quality and comfort to the existing wide body turbofans. This is a technology area that was not discussed in this paper, however, an effort is currently planned as part of NASA's Advanced Turboprop Program to meet this need.

SYMBOLS

AF   blade activity factor =

$$\frac{100,000}{16} \int_{hub}^{r/R = 1.0} b/D \, (r/R)^3 \, d(r/R)$$

AR   aspect ratio

b   elemental blade chord, cm (in.)

C_{LD} elemental blade design lift coefficient

C_{Li} integrated design lift coefficient

$$= 4 \int_{hub}^{r/R = 1.0} C_{LD} \, (r/R)^3 \, d(r/R)$$

Cp   power coefficient = $P/\rho n^3 D^5$

D   tip diameter, cm (in.)

DOC   direct operating cost

$dCp/d(r/R)$ elemental power coefficient

$$(Cp = \int dCp/d(r/R))$$

$dC_T/d(r/R)$ elemental thrust coefficient

$$(C_T = \int dC_T/d(r/R))$$

J   advance ratio, V_o/nD

M_ℓ local Mach number

M_o freestream Mach number

n   rotational speed, revolutions per second

P   power, kW (ft-lb/sec)

PTR	propeller test rig
r	radius, cm (in.)
R	blade tip radius, cm (in.)
SHP	shaft power, kW (ft-lb/sec)
SR	single rotation
T	thrust, Newtons (lb)
t	elemental blade thickness, cm (in.)
V	local velocity, m/sec (ft/sec)
V_o	freestream velocity, m/sec (ft/sec)
x	axial distance, cm (in.)
$\beta\,3/4$	blade angle at 75 percent radius, deg.
$\Delta\beta$	effective blade twist, deg.
η_i	ideal propulsive efficiency = $(T_{ideal} \cdot V_o)/SHP$ (excludes blade profile drag and compressibility losses)
$\eta_{installed}$	installed efficiency = $((T-D)_{installed} \cdot V_o)/SHP$ (installed thrust minus drag of aircraft)
η_{net}	net efficiency = $(T_{net} \cdot V_o)/SHP$ (thrust corrected for buoyance effects)

REFERENCES

1. G. Kraft and W. Strack, "Preliminary Study of Advanced Turboprops for Low Energy Consumption." NASA TM X-71740, 1975.

2. "Energy Consumption Characteristics of Transports Using the Prop-Fan Concept." D6-75780, Boeing Commercial Airplane Co., October 1976; also NASA CR-137937.

3. R. Hirschkron and R. E. Neitzel, "Alternative Concepts for Advanced Energy Conservative Transport Engines." SAE Paper 760536-SAE Air Transportation Meeting, May 1976.

4. R. E. Neitzel, R. Hirschkron, and R. P. Johnston, "Study of Unconventional Aircraft Engines Designed for Low Energy Consumption." R76AEG597, General Electric Co., December 1976; also NASA CR-135136.

5. D. E. Gray and J. W. Witherspoon, "Fuel Conservative Propulsion Concepts for Future Air Transports." SAE Paper 760535-SAE Air Transportation Meeting, May 1976.

6. D. E. Gray, "Study of Unconventional Aircraft Engines Designed for Low Energy Consumption." PWA-5434, Pratt and Whitney Aircraft, June 1976; also NASA CR-135065.

7. J. A. Stern, "Aircraft Propulsion - a Key to Fuel Conservation: An Aircraft Manufacturer's View." SAE Paper 760538-SAE Air Transportation Meeting, May 1976.

8. R. L. Foss and J. P. Hopkins, "Fuel Conservative Potential for the Use of Turboprop Powerplants," SAE Paper 760537-SAE Air Transportation Meeting, May 1976.

9. J. P. Hopkins and H. E. Wharton, "Summary Report: Study of the Cost/Benefit Tradeoffs for Reducing the Energy Consumption of the Commercial Air Transportation System," NASA CR-137927, August 1976.

10. J. P. Hopkins and H. E. Wharton, "Final Report: Study of the Cost/Benefit Tradeoffs for Reducing the Energy Consumption of the Commercial Air Transportation System," NASA CR-137926, August 1976.

11. R. E. Coykendall, et al., "Study of Cost/Benefit Tradeoffs for Reducing the Energy Consumption of the Commercial Air Transportation System." United Air Lines, Inc., June 1976; also NASA CR-137891.

12. F. W. Gobetz and A. A. LeShane, "Cost/Benefit Trade-Offs for Reducing the Energy Consumption of Commercial Air Transportation (RECAT)." UTRC-R76-912036-17, United Technologies Research Center, June 1976; also NASA CR-137878.

13. F. W. Gobetz and A. P. Dubin, "Cost/Benefit Trade-Offs for Reducing the Energy Consumption of Commercial Air Transportation: Final Report," NASA CR-137877, June 1976.

14. C. Rohrbach, "A Report on the Aerodynamic Design and Wind Tunnel Test of a Prop-Fan Model." AIAA Paper No. 76-667-AIAA/SAE 12th Propulsion Conference, July 1976.

15. C. Rohrbach and F. B. Metzger, "The Prop-Fan - A New Look in Propulsors," AIAA Paper 75-1208-AIAA/SAE 11th Propulsion Conference, September-October, 1975.

16. R. M. Grose, "Wind Tunnel Studies of the Effects of Blade Thickness Ratio, Camber and Pitch Distribution on the Performance of Model High-Speed Propellers." R-25665-2, United Aircraft Corp., June 1955.

17. J. L. Hess and A. M. O. Smith, "Calculation of Potential Flow About Arbitrary Bodies." Progress in Aeronautical Sciences, Vol. 8, D. Kuchemann, ed., Pergamon Press, 1967, pp. 1-138.

18. Wen L. Chow, Lawrence J. Bober, and Bernard H. Anderson, "Numerical Calculation of Transonic Boattail Flow." NASA TN D-7984, 1975.

19. O. L. Anderson, "User's Manual for a Finite-Difference Calculation of Turbulent Swirling Compressible Flow in Axisymmetric Ducts with Struts and Slot Cooled Walls, Volume I." USAAMRDL-TR-74-50, U.S. Army Air Mobility Research and Development Lab., 1975.

20. Fred W. Steffen, "Cruise Performance of an Isolated 1.15 Pressure Ratio Trubofan Propulsion System Simulator at Mach Numbers from 0.6 to 0.85." NASA TM X-3064, 1974.

21. S. Goldstein, "On the Vortex Theory of Screw Propellers." Royal Soc. (London) Proc. (1929), 440.

22. James E. Crouse, "Computer Program for Definition of Transonic Axial-Flow Compressor Blade Rows." NASA TN D-7345, 1974.

23. Theodore Katsanis, "Fortran Program for Calculating Transonic Velocities on a Blade-to-Blade Stream Surface of a Turbo-Machine." NASA TN D-5427, 1969.

24. John Stack and W. F. Lindsey, "Characteristics of Low-Aspect-Ratio Wings at Supercritical Mach Numbers." NACA Rept 922, 1949.

25. Henry V. Borst, "Summary of Propeller Design Procedures and Data. Volume I - Aerodynamic Design and Installation." Borst (Henry V.) and Associates (USAAMRDL-TR-73-34A-Vol-1; AD-774831), Nov. 1972.

26. John C. Evvard, "Distribution of Wave Drag and Lift in the Vicinity of Wing Tips at Supersonic Speeds" NACA TN-1382, 1947.
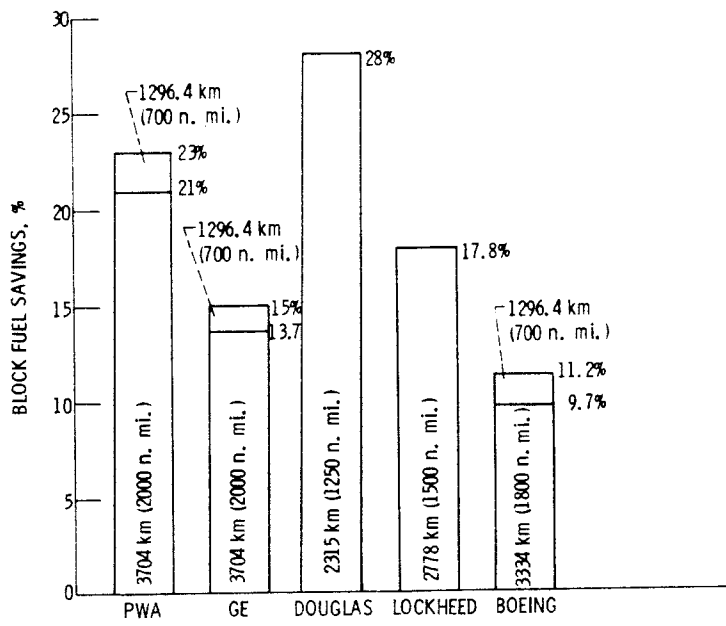
(a) FUEL SAVINGS.
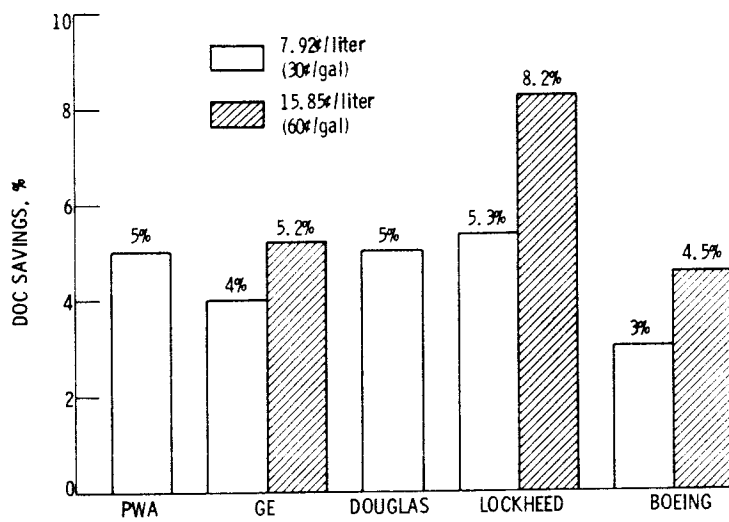
(b) DOC SAVINGS.

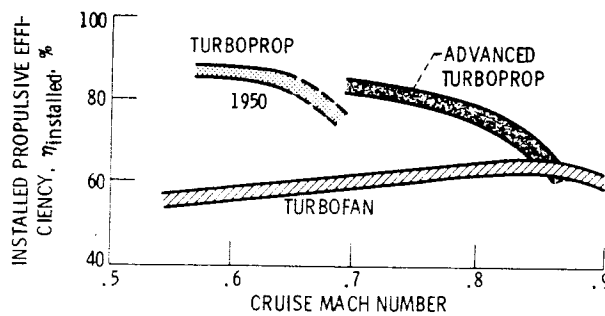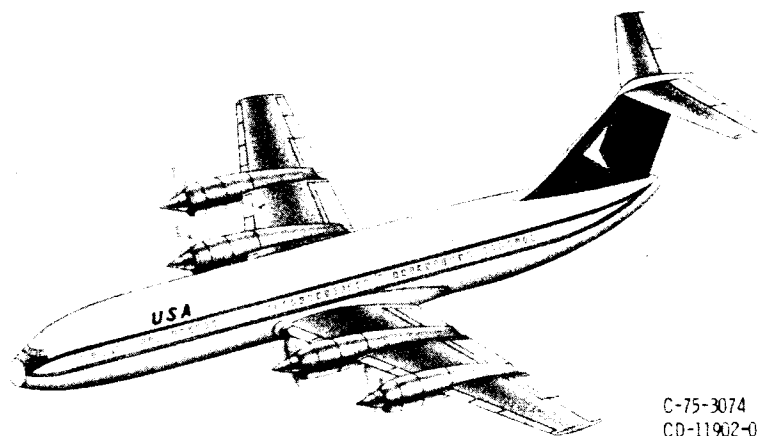Figure 1. - Fuel conservation and DOC study results; M_0 = 0.8 cruise.

Figure 2. - Variation of installed cruise efficiency with Mach number (from ref. 14).

Figure 3. - Advanced low energy turooprop aircraft. Cruise, Mach 0.8;
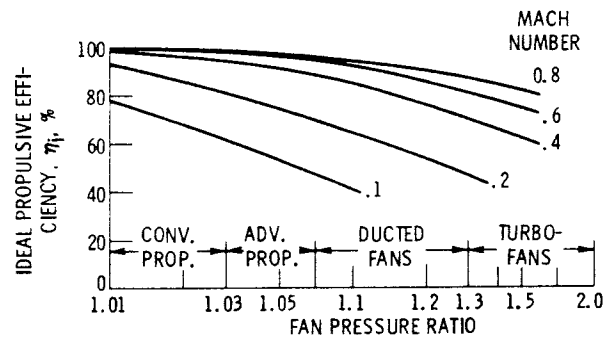10.668 km (35 000 ft).

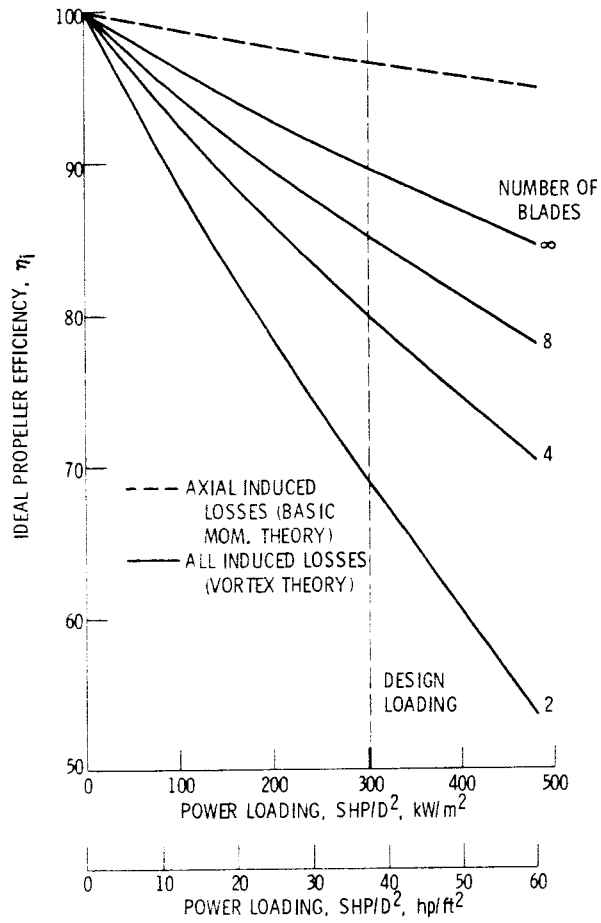Figure 4. - Ideal propulsive efficiency as a function of
fan pressure ratio.

IDEAL PROPELLER EFFICIENCY, η_i

POWER LOADING, SHP/D^2, kW/m^2

NUMBER OF BLADES

∞

8

4

2

DESIGN
LOADING

– – – AXIAL INDUCED
LOSSES (BASIC
MOM. THEORY)
——— ALL INDUCED LOSSES
(VORTEX THEORY)

POWER LOADING, SHP/D^2, hp/ft^2

Figure 5. - Ideal efficiency; 0.8 Mach number at 10.668
km (35 000 ft) altitude and 243.8 m/sec (800 ft/sec) tip
speed.

REDUCED THICKNESS

BLADE SWEEP

NACELLE BLOCKAGE

SPINNER AREA RULING

ADVANCED AIRFOILS
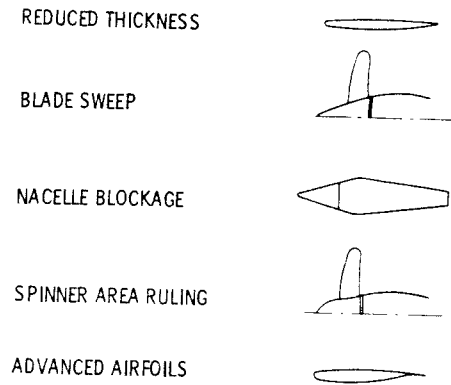
Figure 6. - Advanced aerodynamic concepts for im-
proving propeller performance.

THICKNESS RATIO, t/b

t_3

t_2

t_1

Radius ratio, r/R
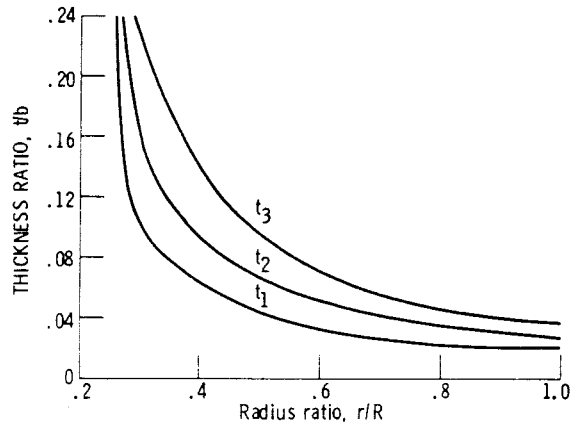
Figure 7. - Thickness ratio distribution of test propellers.
Data source, reference 16.
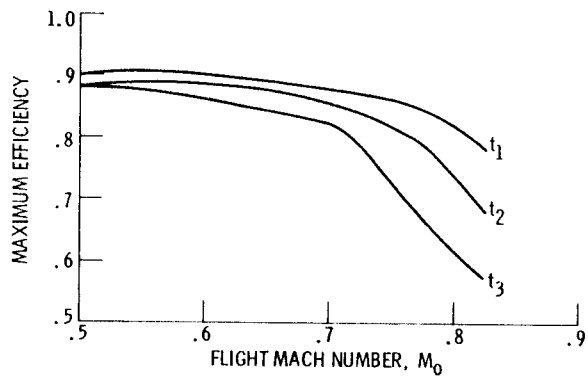
Figure 8. - Variation of maximum efficiency with flight
Mach number and thickness ratio level. Data source,
reference 16.

CURVE

A   SECTION MACH NUMBER, NO VELOCITY
      SUPPRESSION OR SWEEP

B   DRAG DIVERGENCE MACH NUMBER
      (NACA 16-SERIES)

C   SECTION MACH NUMBER WITH 30^0
      TIP SWEEP

D   EFFECTIVE SECTION MACH NUMBER
      (WITH SUPPRESSION AND SWEEP)

M_0 = 0.8, 243.8 m/sec (800 ft/sec) TIP SPEED
8 BLADES, 10.668 km (35 000 ft) ALTITUDE
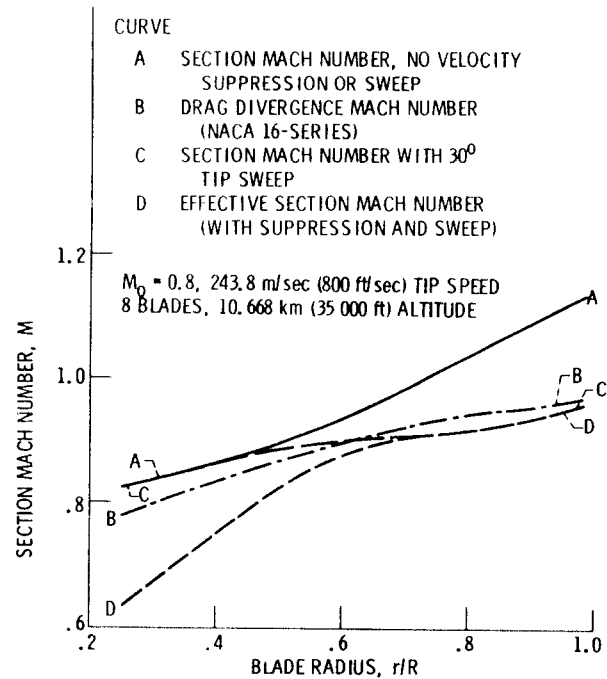
Figure 9. - Typical blade section Mach number distributions.
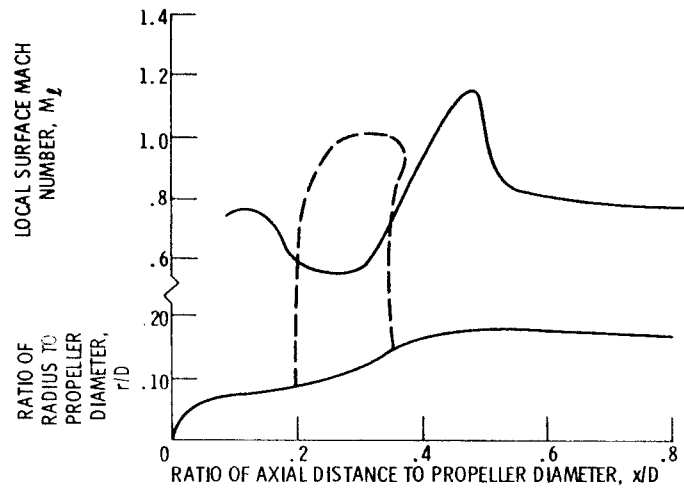
Figure 10. - Body surface Mach number distribution,
M_0 = 0.8.
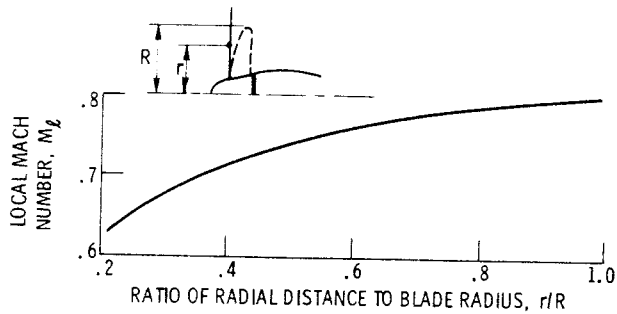
Figure 11. - Radial distribution of local axial Mach number near blade leading edge, $M_0 = 0.8$.
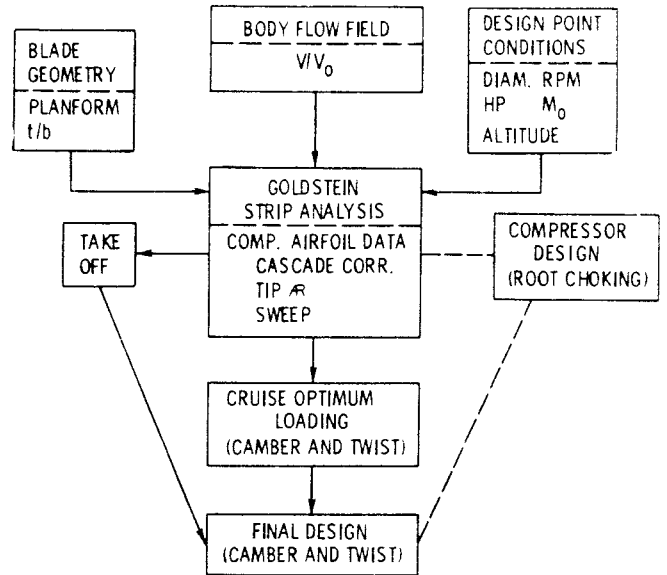
Figure 12. - Advanced propeller design procedure.

8 BLADES/203 AF/0.081 C_{L_i}
HUB TO TIP 0.239 DIA. 62.23 cm (24.5 in.)
DESIGN BLADE ANGLE AT 0.75
RADIUS = 55.8 DEG
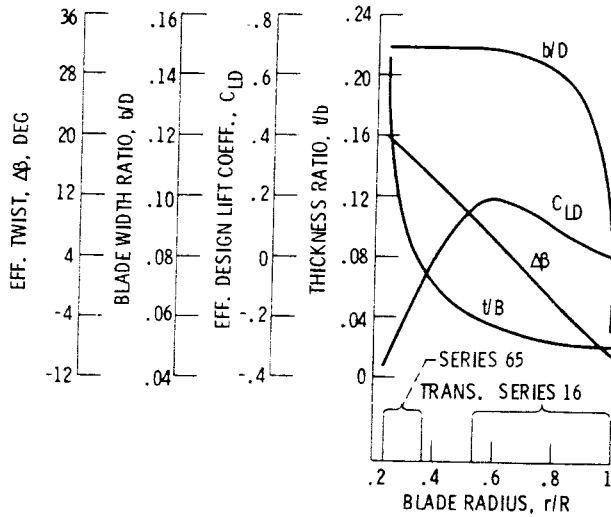
(a) SWEPT BLADE CONFIGURATION, SR-1.
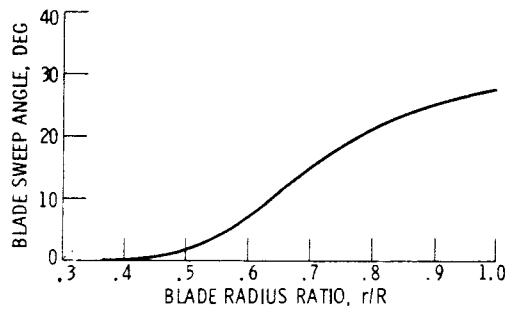
(b) SR-1 BLADE SWEEP DISTRIBUTION.

Figure 13. - Blade characteristics.

8 BLADE/203AF/0.08 C_{L_i}
"STRAIGHT BLADE"
24.5 INCH DIAMETER
DESIGN BLADE ANGLE AT
3/4 RADIUS = 56.7°
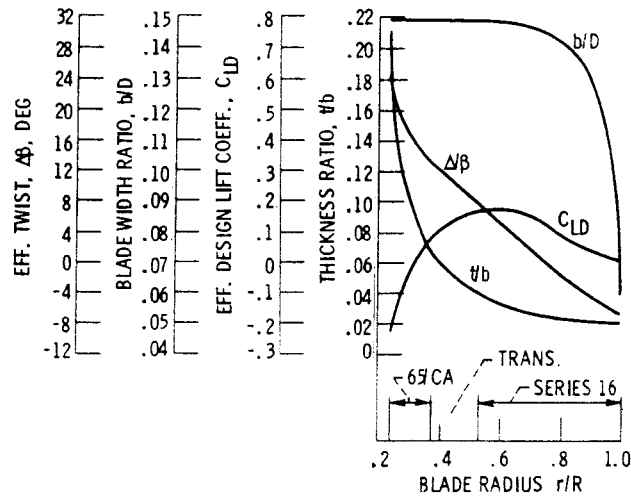
(c) STRAIGHT BLADE CONFIGURATION, SR-2.

Figure 13. - Concluded.

8 BLADES/203 ACTIVITY FACTOR/0.081 CL_i
SHP/D^2 = 301 kW/m² (37.5 hp/ft²) AT 10.668 km (35 000 ft)
0.8 MACH NO.; 243.8 m/sec (800 ft/sec) TIP SPEED
$\eta_{net\ design}$ = 0.795

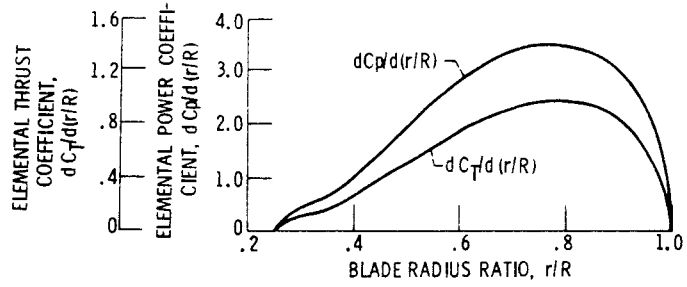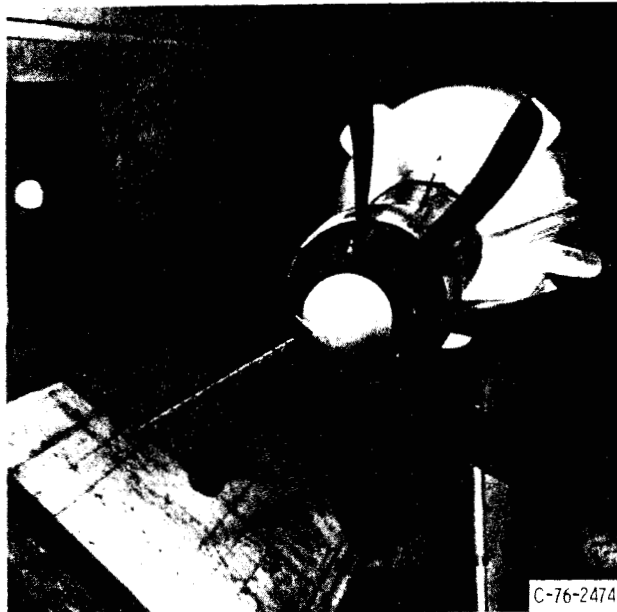Figure 14. - Swept blade thrust and power coefficient loading distributions.

C-76-2474

(a) SR-1, swept blade.

Figure 15. - Propeller models in U.T.R.C. wind tunnel.

C-76-3595

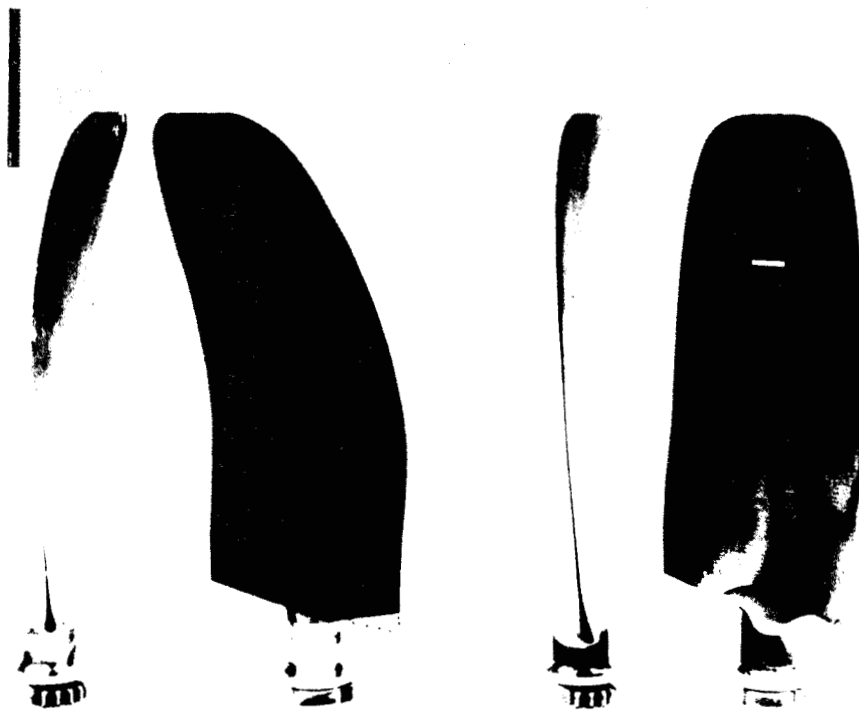(b) SR-2, straight blade with area-ruled hub.

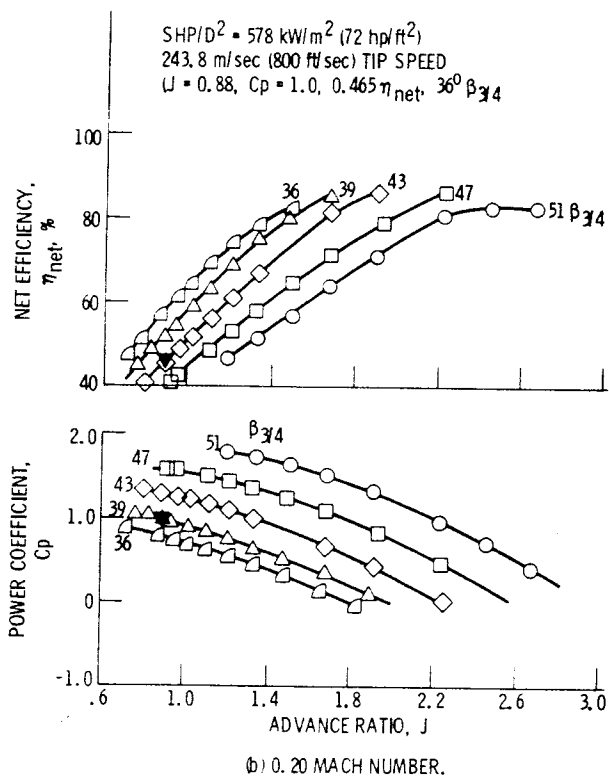Figure 15. - Concluded.
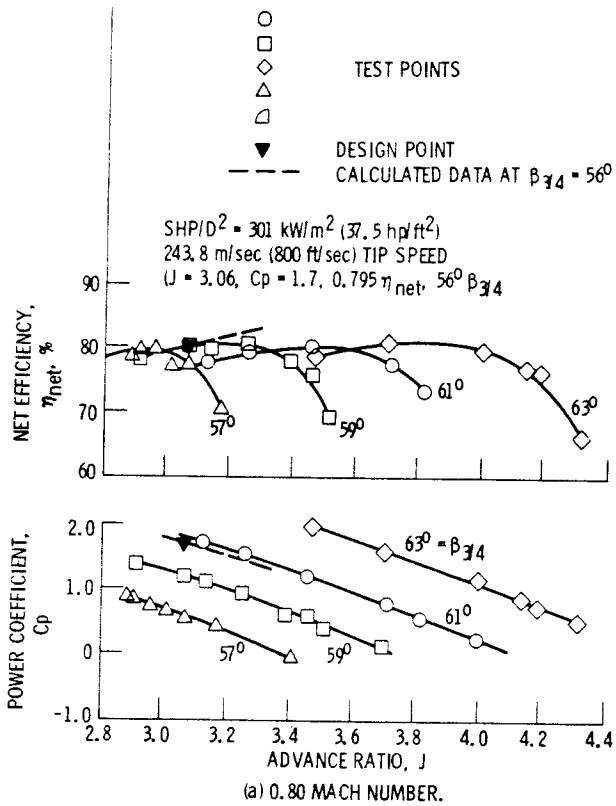
Figure 16. - Propeller model blade comparison.

○
□
◇   TEST POINTS
△
◁

▼   DESIGN POINT
- - -   CALCULATED DATA AT $\beta_{3/4} = 56^\circ$

$SHP/D^2 = 301$ kW/m^2 (37.5 hp/ft^2)
243.8 m/sec (800 ft/sec) TIP SPEED
(J = 3.06, Cp = 1.7, 0.795 η_{net}, 56° $\beta_{3/4}$

NET EFFICIENCY, η_{net}, %

90

80

70

60

61°
57°
59°
63°

2.0

POWER COEFFICIENT, Cp

1.0

0

-1.0

$63^\circ = \beta_{3/4}$
61°
57° 59°

2.8 3.0 3.2 3.4 3.6 3.8 4.0 4.2 4.4
ADVANCE RATIO, J

(a) 0.80 MACH NUMBER.

$SHP/D^2 = 578$ kW/m^2 (72 hp/ft^2)
243.8 m/sec (800 ft/sec) TIP SPEED
(J = 0.88, Cp = 1.0, 0.465 η_{net}, 36° $\beta_{3/4}$

NET EFFICIENCY, η_{net}, %

100

80

60

40

36 39 43 47 51 $\beta_{3/4}$

2.0

POWER COEFFICIENT, Cp

1.0

0

-1.0

$\beta_{3/4}$
51
47
43
39
36

.6 1.0 1.4 1.8 2.2 2.6 3.0
ADVANCE RATIO, J

(b) 0.20 MACH NUMBER.

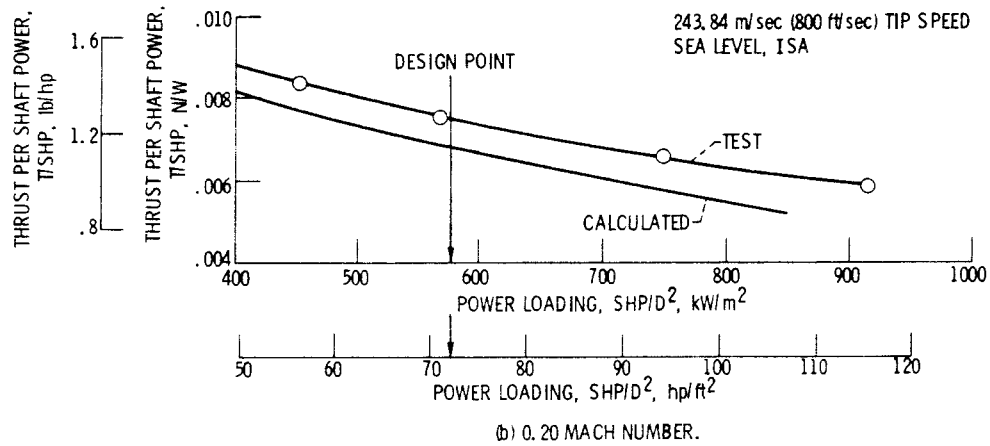Figure 17. - Net efficiency and power coefficient for swept-blade propeller model SR-1.
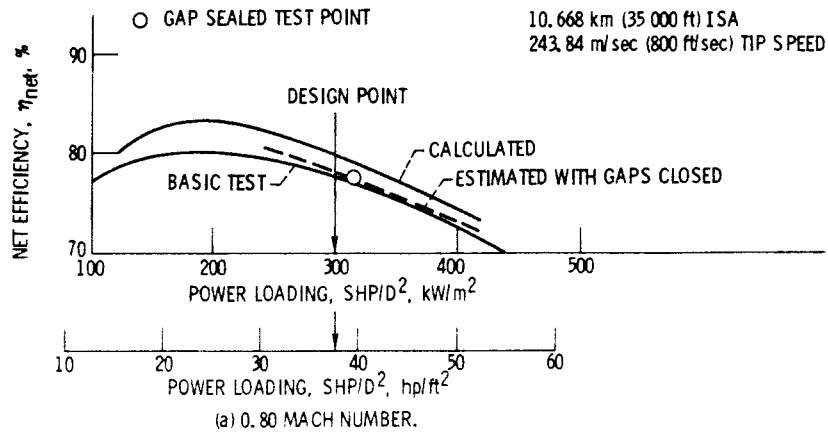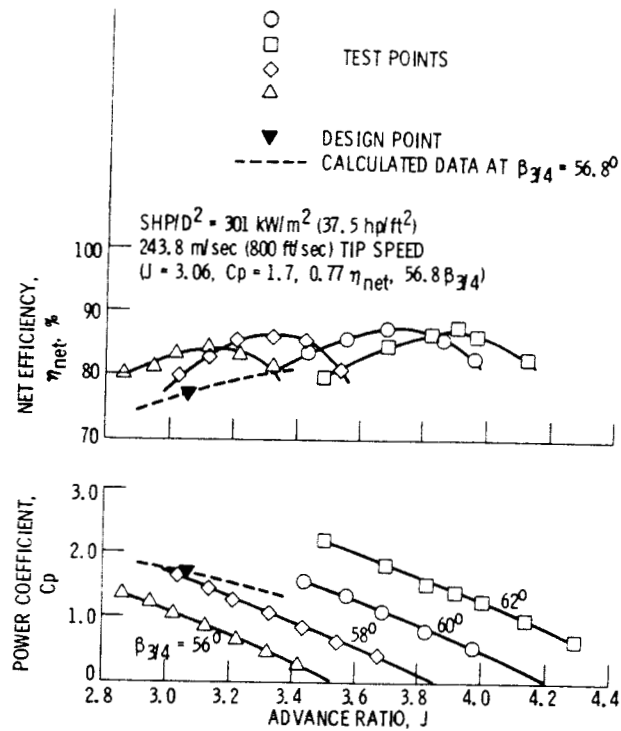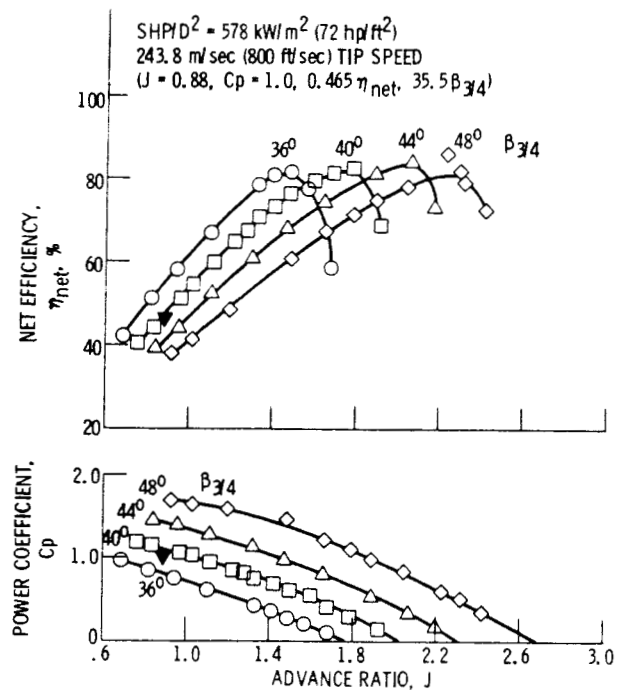
Figure 18. - Variation of net efficiency with power loading.

(a) 0.80 MACH NUMBER.

(b) 0.20 MACH NUMBER.

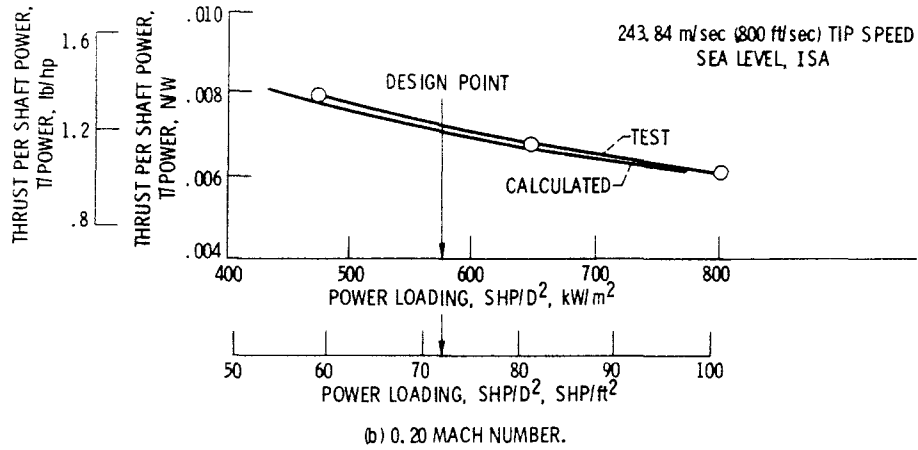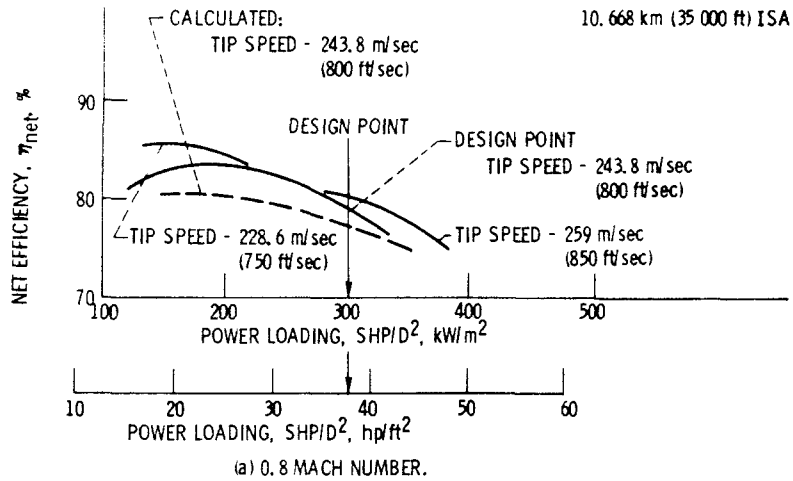Figure 19. – Net efficiency and power coefficient for straight-blade propeller model SR-2.

(a) 0.8 MACH NUMBER.

(b) 0.20 MACH NUMBER.

Figure 20. - Variation of net efficiency and thrust per shaft power with power loading for straight-blade propeller SR-2.

	DESIGN $C_p = 1.7$, $J = 3.06$ $V_{tip} = 243.8$ m/sec (800 ft/sec)				OFF-DESIGN $C_p = 1.41$, $J = 2.88$ $V_{tip} = 259$ m/sec (850 ft/sec)
	BLADE ANGLE, $\beta_{3/4}$		NET EFF., η_{net}		NET EFF., η_{net}
CONFIG.	ANAL.	EXP.	ANAL.	EXP.	EXP.
SR-1 (SWEPT)	56.0°	~61°	79.5%*	78.2%	------
SR-2 (STRAIGHT)	56.8°	~58°	77.0%	78.8%	80.2%

*VALUE USED IN MISSION ANALYSIS STUDIES.

Figure 21. - Performance summary 0.8 Mach number. $SHP/D^2 = 301$ kW/m² (37.5 hp/ft²).

UPDATED ANALYSIS

REVISED TWIST

BLADE ROOT FAIRING AND SEALING

IMPROVED SWEEP

ADVANCED BLADE SECTIONS (SUPERCRITICAL)

IMPROVED SPINNER AREA RULING

IMPROVED THICKNESS DISTRIBUTION

INCREASED BLADE NUMBER

LOWER POWER LOADING

COUNTER ROTATION

Figure 22. - Potential performance improvements.

Figure 23. - Lewis PTR in 8-by 6-foot supersonic wind tunnel.